

Coherent beam combining of high power broad-area laser diode array with near diffraction limited beam quality and high power conversion efficiency

B. Liu^{1,2,*} and Y. Braiman^{1,2}

¹Center for Engineering Science Advanced Research, Computer Science & Mathematics Division, Oak Ridge National Laboratory, Oak Ridge, Tennessee 37831, USA

²Department of Mechanical, Aerospace, and Biomedical Engineering, University of Tennessee, Knoxville, Tennessee 37996, USA

*liub@ornl.gov

Abstract: We explored a path of achieving high quality phase-locking of broad-area laser diode (BALD) array that operates at high electrical to optical power conversion efficiency (PCE). We found that (a) improving single transverse mode control for each individual BALD, (b) employing global Talbot optical coupling among diodes, and (c) enhancing strength of optical coupling among diodes are key factors in achieving high quality phase-locking of high power BALD array. Subsequently, we redesigned and improved a V-shaped external Talbot cavity and employed low reflectivity anti-reflection (AR) coated, low-“smile” BALD array to meet these three important requirements. We demonstrated near-diffraction limit far-field coherent pattern with 19% PCE and 95% visibility. The far-field angle (full-width at half-maximum (FWHM)) of center lobe was measured as 1.5 diffraction angular limited with visibility of 99% for 5A injection current and 1.6 diffraction angular limited with visibility of 95% for 14A injection current. Power scaling of diode array is discussed.

©2013 Optical Society of America

OCIS codes: (140.2010) Diode laser arrays; (140.3298) Laser beam combining; (140.3300) Laser beam shaping; (140.3410) Laser resonators.

References and links

1. T. Y. Fan, “Laser beam combining for high-power, high-radiance sources,” *IEEE J. Sel. Top. Quantum Electron.* **11**(3), 567–577 (2005).
2. L. Bartelt-Berger, U. Brauch, A. Giesen, H. Huegel, and H. Opower, “Power-scalable system of phase-locked single-mode diode lasers,” *Appl. Opt.* **38**(27), 5752–5760 (1999).
3. T. M. Shay, V. Benham, J. T. Baker, B. Ward, A. D. Sanchez, M. A. Culpepper, D. Pilkington, J. Spring, D. J. Nelson, and C. A. Lu, “First experimental demonstration of self-synchronous phase locking of an optical array,” *Opt. Express* **14**(25), 12015–12021 (2006).
4. W. Liang, A. Yariv, A. Kewitsch, and G. Rakuljic, “Coherent combining of the output of two semiconductor lasers using optical phase-lock loops,” *Opt. Lett.* **32**(4), 370–372 (2007).
5. E. C. Cheung, J. G. Ho, G. D. Goodno, R. R. Rice, J. Rothenberg, P. Thielen, M. Weber, and M. Wickham, “Diffraction-optics-based beam combination of a phase-locked fiber laser array,” *Opt. Lett.* **33**(4), 354–356 (2008).
6. S. M. Redmond, K. J. Creedon, J. E. Kinsky, S. J. Augst, L. J. Missaggia, M. K. Connors, R. K. Huang, B. Chann, T. Y. Fan, G. W. Turner, and A. Sanchez-Rubio, “Active coherent beam combining of diode lasers,” *Opt. Lett.* **36**(6), 999–1001 (2011).
7. K. J. Creedon, S. M. Redmond, G. M. Smith, L. J. Missaggia, M. K. Connors, J. E. Kinsky, T. Y. Fan, G. W. Turner, and A. Sanchez-Rubio, “High efficiency coherent beam combining of semiconductor optical amplifiers,” *Opt. Lett.* **37**(23), 5006–5008 (2012).
8. J. R. Leger, M. L. Scott, and W. B. Veldkamp, “Coherent addition of AlGaAs lasers using microlenses and diffractive coupling,” *Appl. Phys. Lett.* **52**(21), 1771–1773 (1988).
9. D. Mehuys, K. Mitsunaga, L. Eng, W. K. Marshall, and A. Yariv, “Supermode control in diffraction-coupled semiconductor laser arrays,” *Appl. Phys. Lett.* **53**(13), 1165–1167 (1988).

10. D. Botez, L. J. Mawst, G. Peterson, and T. J. Roth, "Resonant optical transmission and coupling in phase locked diode laser arrays of antiguides: the resonant optical waveguide array," *Appl. Phys. Lett.* **54**(22), 2183–2185 (1989).
11. F. X. D'Amato, E. T. Siebert, and C. Roychoudhuri, "Coherent operation of an array of diode lasers using a spatial filter in a Talbot cavity," *Appl. Phys. Lett.* **55**(9), 816–818 (1989).
12. D. Botez, L. J. Mawst, G. L. Peterson, and T. J. Roth, "Phase-locked arrays of antiguides: modal content and discrimination," *IEEE J. Quantum Electron.* **26**(3), 482–495 (1990).
13. D. Botez, M. Jansen, L. J. Mawst, G. Peterson, and T. J. Roth, "Watt-range, coherent, uniphase powers from phase-locked arrays of antiguided diode lasers," *Appl. Phys. Lett.* **58**(19), 2070–2072 (1991).
14. R. Waarts, D. Mehuys, D. Nam, D. Welch, W. Streifer, and D. Scifres, "High-power, cw, diffraction-limited, GaAlAs laser diode array in an external Talbot cavity," *Appl. Phys. Lett.* **58**(23), 2586–2588 (1991).
15. L. J. Mawst, D. Botez, C. Zmudzinski, M. Jansen, C. Tu, T. J. Roth, and J. Yun, "Resonant self-aligned-stripe antiguided diode laser array," *Appl. Phys. Lett.* **60**(6), 668–670 (1992).
16. C. J. Corcoran and F. Durville, "Experimental demonstration of a phase-locked laser array using a self-Fourier cavity," *Appl. Phys. Lett.* **86**(20), 201118 (2005).
17. I. Hassiaoui, N. Michel, G. Bourdet, R. Mc Bride, M. Lecomte, O. Parillaud, M. Calligaro, M. Krakowski, and J. P. Huignard, "Very compact external cavity diffraction-coupled tapered laser diodes," *Appl. Opt.* **47**(6), 746–750 (2008).
18. D. Paboeuf, G. Lucas-Leclin, P. Georges, N. Michel, M. Krakowski, J. Lim, S. Sujecki, and E. Larkins, "Narrow-line coherently combined tapered laser diodes in a Talbot external cavity with a volume Bragg grating," *Appl. Phys. Lett.* **93**(21), 211102 (2008).
19. R. K. Huang, B. Chann, L. J. Missagia, S. J. Augst, M. K. Connors, G. W. Turner, A. Sanchez-Rubio, J. P. Donnelly, J. L. Hostetler, C. Miester, and F. Dorsch, "Coherent combination of slab-coupled optical waveguide lasers," *Proc. SPIE* **7230**, 72301G (2009).
20. S. M. Redmond, D. J. Ripin, C. X. Yu, S. J. Augst, T. Y. Fan, P. A. Thielen, J. E. Rothenberg, and G. D. Goodno, "Diffraction coherent combining of a 2.5 kW fiber laser array into a 1.9 kW Gaussian beam," *Opt. Lett.* **37**(14), 2832–2834 (2012).
21. Y. Zhao, J. Fan, and L. Zhu, "Modal and scalability analysis of a zigzag array structure for passive coherent beam combining," *J. Opt. Soc. Am. B* **29**(4), 650–655 (2012).
22. R. Roy and K. S. Thornburg, Jr., "Experimental synchronization of chaotic lasers," *Phys. Rev. Lett.* **72**(13), 2009–2012 (1994).
23. M. C. Soriano, J. Garcia-Ojalvo, C. R. Mirasso, and I. Fischer, "Complex photonics: dynamics and applications of delay-coupled semiconductor lasers," *Rev. Mod. Phys.* **85**(1), 421–470 (2013).
24. D. Botez, L. J. Mawst, A. Bhattacharya, J. Lopez, J. Li, T. F. Kuech, V. P. Iakovlev, G. I. Suruceanu, A. Caliman, and A. V. Syrbu, "66% CW wallplug efficiency from Al-free 0.98 μm -emitting diode lasers," *Electron. Lett.* **32**(21), 2012 (1996).
25. M. Kanskar, T. Earles, T. J. Goodnough, E. Sties, D. Botez, and L. J. Mawst, "73% CW power conversion efficiency at 50 W from 970 nm diode laser bars," *Electron. Lett.* **41**(5), 245 (2005).
26. C. J. Chang-Hasnain, J. Berger, D. R. Scifres, W. Streifer, J. R. Whinnery, and A. Dienes, "High power with high efficiency in a narrow single-lobed beam from a diode laser array in an external cavity," *Appl. Phys. Lett.* **50**(21), 1465–1467 (1987).
27. L. Goldberg and J. F. Weller, "Narrow lobe emission of high-power broad strip laser in external resonator cavity," *Electron. Lett.* **25**(2), 112–114 (1989).
28. R. M. R. Pillai and E. M. Garmire, "Paraxial-misalignment insensitive external-cavity semiconductor-laser array emitting near-diffraction limited single-lobed beam," *IEEE J. Quantum Electron.* **32**(6), 996–1008 (1996).
29. D. Stryckman, G. Rousseau, M. D'Auteuil, and N. McCarthy, "Improvement of the lateral-mode discrimination of broad-area diode lasers with a profiled reflectivity output facet," *Appl. Opt.* **35**(30), 5955–5959 (1996).
30. S. Wolff, D. Messerschmidt, and H. Fouckhardt, "Fourier-optical selection of higher order transverse modes in broad area lasers," *Opt. Express* **5**(3), 32–37 (1999).
31. S. Wolff and H. Fouckhardt, "Intracavity stabilization of broad area lasers by structured delayed optical feedback," *Opt. Express* **7**(6), 222–227 (2000).
32. S. Mailhot, Y. Champagne, and N. McCarthy, "Single-mode operation of a broad-area semiconductor laser with an anamorphic external cavity: experimental and numerical results," *Appl. Opt.* **39**(36), 6806–6813 (2000).
33. V. Raab and R. Menzel, "External resonator design for high-power laser diodes that yields 400mW of TEM₀₀ power," *Opt. Lett.* **27**(3), 167–169 (2002).
34. V. Raab, D. Skoczowsky, and R. Menzel, "Tuning high-power laser diodes with as much as 0.38 W of power and $M^2 = 1.2$ over a range of 32 nm with 3-GHz bandwidth," *Opt. Lett.* **27**(22), 1995–1997 (2002).
35. S. K. Mandre, I. Fischer, and W. Elsässer, "Control of the spatiotemporal emission of a broad-area semiconductor laser by spatially filtered feedback," *Opt. Lett.* **28**(13), 1135–1137 (2003).
36. J. Chen, X. D. Wu, J. H. Ge, A. Hermerschmidt, and H. J. Eichler, "Broad-area laser diode with 0.02 nm bandwidth and diffraction limited output due to double external cavity feedback," *Appl. Phys. Lett.* **85**(4), 525–527 (2004).
37. E. Samsøe, P. E. Andersen, S. Andersson-Engels, and P. M. Petersen, "Improvement of spatial and temporal coherence of a broad area laser diode using an external-cavity design with double grating feedback," *Opt. Express* **12**(4), 609–616 (2004).
38. A. Jechow, V. Raab, R. Menzel, M. Cenkier, S. Stry, and J. Sacher, "1 W tunable near diffraction limited light from a broad area laser diode in an external cavity with a line width of 1.7 MHz," *Opt. Commun.* **277**(1), 161–165 (2007).

39. B. Liu, Y. Liu, and Y. Braiman, "Coherent addition of high power laser diode array with a V-shape external Talbot cavity," *Opt. Express* **16**(25), 20935–20942 (2008).
40. B. Liu, Y. Liu, and Y. Braiman, "Coherent beam combining of high power broad-area laser diode array with a closed-V-shape external Talbot cavity," *Opt. Express* **18**(7), 7361–7368 (2010).
41. B. Chann, I. Nelson, and T. G. Walker, "Frequency-narrowed external-cavity diode-laser-array bar," *Opt. Lett.* **25**(18), 1352–1354 (2000).
42. E. Babcock, B. Chann, I. A. Nelson, and T. G. Walker, "Frequency-narrowed diode array bar," *Appl. Opt.* **44**(15), 3098–3104 (2005).
43. B. Liu, Y. Liu, and Y. Braiman, "Linewidth reduction of a broad-area laser diode array in a compound external cavity," *Appl. Opt.* **48**(2), 365–370 (2009).
44. N. U. Wetter, "Three-fold effective brightness increase of laser diode bar emission by assessment and correction of diode array curvature," *Opt. Laser Technol.* **33**(3), 181–187 (2001).
45. L. Hildebrandt, R. Knispel, S. Stry, J. R. Sacher, and F. Schael, "Antireflection-coated blue GaN laser diodes in an external cavity and Doppler-free indium absorption spectroscopy," *Appl. Opt.* **42**(12), 2110–2118 (2003).
46. I. P. Kaminov, G. Eisenstein, and L. W. Stulz, "Measurement of the modal reflectivity of an antireflection coating on a superluminescent diode," *IEEE J. Quantum Electron.* **19**(4), 493–495 (1983).
47. D. Mehuys, W. Streifer, R. G. Waarts, and D. F. Welch, "Modal analysis of linear Talbot-cavity semiconductor lasers," *Opt. Lett.* **16**(11), 823–825 (1991).
48. J. K. Butler, D. E. Ackley, and D. Botez, "Coupled-mode analysis of phase-locked injection-laser arrays," *Appl. Phys. Lett.* **44**(3), 293–295 (1984).
49. D. Pabeuf, D. Vijayakumar, O. B. Jensen, B. Thestrup, J. Lim, S. Sujecki, E. Larkins, G. Lucas-Leclin, and P. Georges, "Volume Bragg grating external cavities for the passive phase locking of high-brightness diode laser arrays: theoretical and experimental study," *J. Opt. Soc. Am. B* **28**(5), 1289–1299 (2011).
50. D. Pabeuf, F. Emaury, S. de Rossi, R. Mercier, G. Lucas-Leclin, P. Georges, and P. Georges, "Coherent beam superposition of ten diode lasers with a Dammann grating," *Opt. Lett.* **35**(10), 1515–1517 (2010).
51. J. F. Monjardin, K. M. Nowak, H. J. Baker, and D. R. Hall, "Correction of beam errors in high power laser diode bars and stacks," *Opt. Express* **14**(18), 8178–8183 (2006).
52. N. Trella, H. J. Baker, J. J. Wendland, and D. R. Hall, "Dual-axis beam correction for an array of single-mode diode laser emitters using a laser-written custom phase-plate," *Opt. Express* **17**(26), 23576–23581 (2009).
53. N. Trella, H. J. Baker, and D. R. Hall, "Locking and wavelength selection of an ultra-collimated single-mode diode laser bar by a volume holographic grating," *Opt. Express* **21**(4), 4512–4517 (2013).

1. Introduction

Laser beam combining provides a path to simultaneously scale up power, increase brightness and reduce thermal burden in laser arrays [1]. Coherent beam combining of lasers is an appealing technology in designing high power coherent laser source. Coherent laser source can be useful in a variety of applications such as directed energy, free-space optical communication, and nonlinear optics processes including high-efficiency blue-green light generation.

Locking phases of lasers is a key step to achieve coherent beam combining. Phase locking designs can be grouped into two categories: active phase locking and passive phase locking. The master-oscillator power amplifier (MOPA) design is extensively used in active phase locking approach. In MOPA design, the center wavelength of each individual amplifier channel is locked by optical injection from master oscillator. Phase adjustments of each channel are limited by the response bandwidth of feedback control electronics [2–7]. Passive phase locking employs optical coupling among lasers in either monolithic chip or external cavity. As a result, lasers oscillate in a collective coupled-mode pattern [8–21]. It was demonstrated that phases of chaotic lasers can be locked together due to optical coupling and optical coupling retains broad response bandwidth [22, 23]. Proper optical coupling with strong collective mode discrimination is the key for a successful passive phase locking. External Talbot cavity imposes diffraction feedback coupling with strong collective mode discrimination and therefore was successfully utilized for coherent beam combining of single mode laser diode (LD) array [8, 9, 11]. The combined power was limited by the number of phase locked LDs and the power of each LD. Increasing the power of an individual single LD is a plausible path to increase coherent output power. Two approaches (tapered laser diode and slab-coupled optical waveguide laser (SCOWL)) were implemented to increase the output power of single LD with well-defined transverse mode. Coherent beam combining of a tapered LD array and SCOWL array with external Talbot cavity was investigated in references [17–19].

Commercial broad-area laser diode (BALD) emits high optical power with high PCE ranged from 50% to 70% [24, 25]. The cost of BALD is low since the fabrication of BALD is relatively simple. However, wide emitter size reduces transverse mode discrimination and low mode discrimination results in multi-transverse mode oscillations and consequently low beam quality. Limiting the number of BALD transverse modes constitutes a path of increasing the beam quality of BALD. Applying low anti-reflection (AR) coating to a BALD and employing external optical feedback to a BALD can limit the number of transverse modes. A variety of external feedback designs can limit the number of transverse modes of BALD and improve the beam quality [26–38]. The off-axis optical feedback was introduced to enhance one transverse mode and significantly increase beam quality of BALD [33, 34, 36, 38].

Recently, the off-axis external cavity and Talbot external cavity were combined together to form a V-shaped external Talbot cavity [39, 40]. Coherent beam combining from an array consisting of 47 BALDs was demonstrated. Such array emitted 12.8 Watts output power [40]. However the PCE of coherent beam combining array was in the range of 12% and the far-field angular distribution was a couple of times larger than diffraction limited. This PCE was lower than the values demonstrated for coherent beam combination of tapered LD array external Talbot cavity (estimated ~18%) and SCOWL array external Talbot cavity (estimated ~22%) [18, 19]. Near diffraction angular limit far-field was demonstrated with tapered LD array external Talbot cavity [18]. An important question can be asked: is it possible to design an external cavity that make possible high PCE operation (in the range of 20%) and near diffraction limit far field emission from a BALD array?

In this paper, we explored a path of achieving high quality passive phase-locking of high-power BALD array with near diffraction angular limit far-field and high PCE. We found that (a) improving single transverse mode control for each individual BALD on array, (b) implementing global Talbot optical coupling among diodes, and (c) enhancing strength of optical coupling among diodes are key factors in achieving high quality phase-lock high power BALD. To meet these three important requirements, we redesigned and improved a V-shaped external Talbot cavity and employed low reflectivity anti-reflection (AR) coated, low-“smile” BALD array. Low reflectivity AR-coating allows external cavity to have better mode selection. Design-improved V-shaped external Talbot cavity (a telescope along fast-axis matched with fast-axis-collimation (FAC) (NA = 0.8)) narrows spectral line-width and reduces the “smile effect”. Low-“smile” BALD array subject to design-improved V-shaped external Talbot cavity allows sufficient optical coupling among diodes. Therefore the design-improved V-shaped external Talbot cavity increases the diffraction coupling among diodes. We implemented design-improved V-shaped external Talbot cavity with an array of 10 BALDs and demonstrated PCE in the range of 19% while maintaining coherent beam with well-maintained coherence (95% visibility). The near-diffraction angular limited far-field pattern was demonstrated and compared with the numerical simulation of far-field pattern from in-phase locked 10 LDs. The far-field angle (full-width at half-maximum (FWHM)) of center lobe was measured as 1.5 diffraction angular limited with visibility of 99% for 5 A injection current and 1.6 diffraction angular limited with visibility of 95% for 14 A injection current.

2. Experiment

PCE of BALD with single transverse mode emission ranges from approximately 9.5% ($M^2 \sim 1.03$) to 17.6% ($M^2 \sim 2.57$) [33]. With diffractive grating loaded external cavity, the demonstrated PCE was even lower and was estimated to be approximately 5% (200 mW, 2A) with $M^2 \sim 1.3$ and laser spectrum line-width ~ 8 pm [34]. In order to suppress the intrinsic BALD mode oscillation and increase PCE of the single transverse mode emission, the AR-coating with lower reflectivity is needed. High PCE (estimated as ~17%) was achieved with high quality beam ($M^2 \sim 1.3$) and narrow spectrum line-width (~ 2 MHz) using high-quality AR-coated ($R < 10^{-5}$) BALD [38]. This result indicates that low reflectivity AR-coating plays an important role in improving the beam quality and in increasing the PCE.

In the past decade, driven by the need to design high power narrow spectral line-width lasers, external cavity designs of BALD array were extensively studied [41, 42]. Due to non-ideal packaging, the vertical positions of diodes normally show “smile” distribution. Non-identical vertical positions of diodes (“smile”) cause variations of laser beam angles incident to gratings by collimation optics. As a result, each individual laser diode has different spectrum (the smile effect was analyzed in detail [41, 43]). Since optical coupling among diodes placed in external Talbot cavity is realized due to grating reflection, array “smile” significantly reduces optical coupling among diodes. B. Chann *et. al.*, proposed and implemented telescope optics to reduce the smile effect narrowing spectral line-width [41, 42].

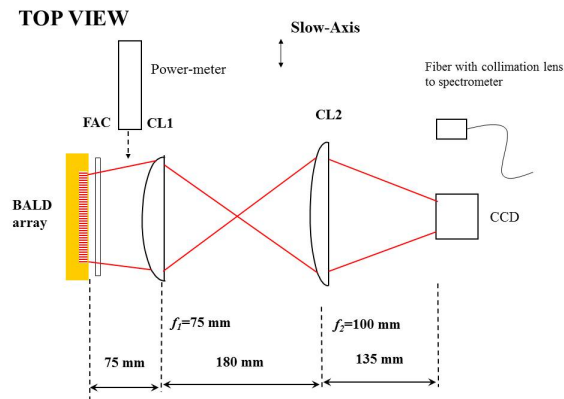


Fig. 1. Experimental schematic design for BALD array smile, free-running spectrum, and free-running L-I curve measurements.

Since our experiment requires strong transverse mode control and strong optical coupling among diodes, it is important to use a small smile and low reflectivity AR-coated BALD array. We setup an experiment to measure the smile and estimate the AR-coating reflectivity. The experimental schematic design is shown in Fig. 1 and it is similar to Wetter’s design [44]. The laser beam of BALD array was collimated by FAC (NA = 0.8, $f = 1.3$ mm). Two cylindrical lenses (CL1, CL2) composed of image optics along slow-axis with focal length 75 mm and 100 mm, respectively. One neutral density filter (is not shown in Fig. 1) was used to attenuate the intensity of laser. The image of BALD array was recorded by CCD camera. Our BALD array was manufactured by LaserTel. It is comprised of 10 BALDs with 100 μm wide emitter and the pitch of array 200 μm . The residual AR-coating reflectivity of BALD array was estimated as 0.5% by the manufacturer. The center wavelength of gain profile was around 800 nm.

We tested a set of 5 BALD arrays consisting of 10, 25, and 49 BALDs each. The smile of array of 10 BALDs, 25 BALDs, and 49 BALDs is approximately 0.25 μm , 1 μm , 2~3 μm , respectively. In order to demonstrate good optical coupling among diodes in our experiment, we selected an array of 10 BALDs with lower smile. The best experimental results (the smallest smile and the highest threshold) are shown in Fig. 2. The near-field image is shown in Fig. 2(a). Figure 2(b) shows the intensity of 10 BALDs with 3 Amps current drive. Figure 2(c) shows a broad luminescence spectrum of 15.5 nm (FWHM) with 3 Amps current drive. The threshold of our AR-coating BALD array is around 7 Amps while the threshold of a standard AR-coated BALD array is 3.5 A. By comparing with Fig. 4 in [45], we estimated that the residual reflectivity of this AR-coating was about 0.1%~0.2%. Modulation of superluminescence spectrum was not resolved in our spectrum for two reasons: overlap of multi-laser diode spectra and higher residual reflectivity AR-coating (0.2%) compared to 0.02% in [46].

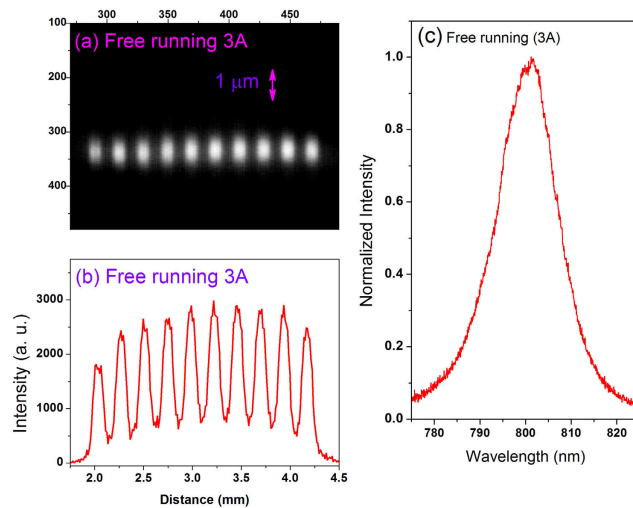


Fig. 2. (a) Near-field of selected BALD array (mini-bar, 10 BALDs) with 3 Amps injection current. BALD array has smile around $0.25 \mu\text{m}$. (b) near-field mode profile of selected BALD array. (c) Solitary BALD array spectrum. A broad luminescence spectrum of 15.5 nm (FWHM) with 3 Amps current drive.

A schematic design of a V-shaped external Talbot cavity that was optimized to address the issues discussed above is shown in Fig. 3. A pair of prism mirrors formed a right angle and separated the laser beam into two paths. The right-side feedback path consisted of cylindrical lenses CL1-CL4 and diffraction grating. A pair of lenses CL2 ($f_2 = 50 \text{ mm}$) and CL3 ($f_3 = 200 \text{ mm}$) comprised a telescope with magnification $M = 4$ along fast-axis direction. It reduced the smile effect and narrowed spectral line-width of BALD array [42]. If we used the external cavity without telescope as shown in [39, 40], the laser beam size on grating along fast-axis was about 2.5 mm . The spectral line-width of BALD array with external cavity was about 0.3 nm . A laser with broad spectral line-width implies short coherence length of a laser and no coherence interference pattern on the far-field. With the telescope configuration shown in Fig. 3, the laser beam on grating along fast-axis was expanded to around 10.0 mm . The spectral line-width of BALD array was around 0.1 nm . Such a design facilitated coherent phase locking of diodes. The transform optics comprised of a pair of confocal lenses CL1 and CL4 ($f_1 = f_4 = 200 \text{ mm}$) projected laser diode image on the focal plane of CL4. Grating was at the half Talbot distance ($Z_t/2$) from CL4 image plane, where $Z_t = 2d^2/\lambda$ is the Talbot distance, λ is the laser wavelength, and d is the array pitch. The first-order diffraction of the laser beam was reflected to laser diodes by diffraction grating (830-line/mm, gold-coating) which was arranged in the Littrow configuration. The blaze angle of grating was about 18° and the diffraction efficiency of first order was more than 85%. External Talbot cavity provided off-axis ($\theta = 2.38^\circ$) feedback. The far-field profile was projected to the focal plane of cylindrical lens CL5 ($f_5 = 300 \text{ mm}$) and recorded by a CCD camera. An optical spectrum analyzer with a sensitivity of 70 pm was used to measure the spectrum while a power meter monitored the output power. Inset 1 in Fig. 3 shows an individual BALD in V-shaped external cavity. The side-view of external Talbot cavity (feedback branch) for the entire array is shown in Fig. 4.

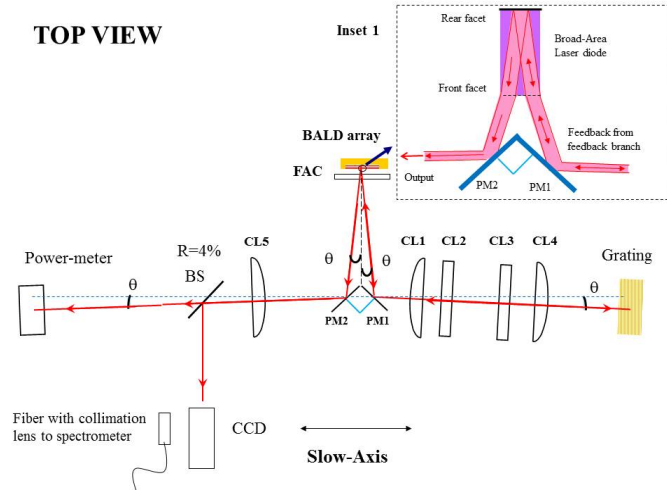


Fig. 3. Schematic design of an improved V-shaped external Talbot cavity BALD array (top view). FAC is fast-axis collimator. Two prism mirrors (PM1, PM2) form right angle and separate the laser beams into two branches (feedback branch and output branch). Feedback branch consists of cylindrical lenses CL1~CL4, and Grating. CL1, CL3, and CL4 are cylindrical lenses with the focal length 200 mm. CL2 is the cylindrical lens with focal length 50 mm. Grating is a ruled diffraction grating with groove density 830 line/mm. CL2 and CL3 form a telescope along fast-axis and expand laser beam 4 times along fast-axis. The confocal lens pair CL1, CL4 project the image laser diodes on the CL4 focal plane. The far-field profile of laser diode array is projected on CL5 ($f_5 = 300$ mm) focal plane. A CCD camera records the far-field profile and optical spectrum analyzer measures the spectrum while a power-meter monitors the output power. Inset 1 shows an individual BALD in V-shaped external cavity.

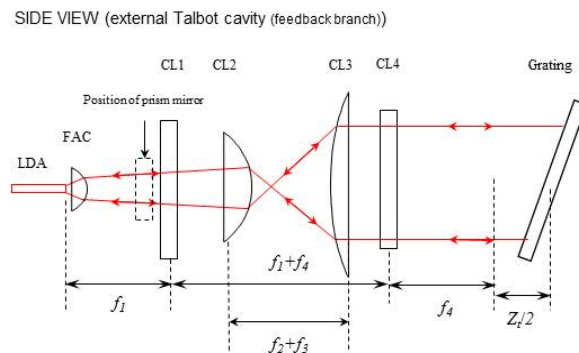


Fig. 4. Feedback branch of optimized V-shaped external Talbot cavity (side view). FAC (NA = 0.8) collimates laser beam along the fast-axis within divergence angle (± 1.5 mrad). Confocal cylindrical lenses CL1 and CL4 ($f_1 = f_4 = 200$ mm) project laser diode image on CL4 focal plane. Telescope comprised of CL2 ($f_2 = 50$ mm) and CL3 ($f_3 = 200$ mm) expands laser beam with 4 times along fast-axis direction. Grating is located at the half Talbot distance from CL4 image plane and provides a self-imaged diffractive-coupling feedback.

3. Results and discussion

In Fig. 5, a CW L-I characteristic of coherent beam combining BALD array with a design-improved V-shaped external Talbot cavity (red dot-line) is presented, accompanied with CW L-I characteristic of the free-running BALD array (black square-line). The V-I curve (magenta triangle-line) is also shown in Fig. 5. For current drive values below 10 Amps, output power of coherent beam combining BALD array with an optimized V-shaped external

cavity is higher than the free running BALD array. High visibility (~95%) interference far-field pattern is maintained up to values of the drive current of 14 Amps. From the V-I curve, we can calculate the total consumed power of BALD array. The PCE is calculated with the output power (L-I curve) over the total consumed power (V-I curve). The calculated PCE (blue diamond-line) is also shown in Fig. 5. The highest calculated PCE of coherent beam combining is around 19%. We noted here that 19% PCE is comparable with the value reported in experiments using single-mode diode array in external Talbot cavity (estimated 18% from tapered LDA and estimated 22% from SCOWL array [18, 19]).

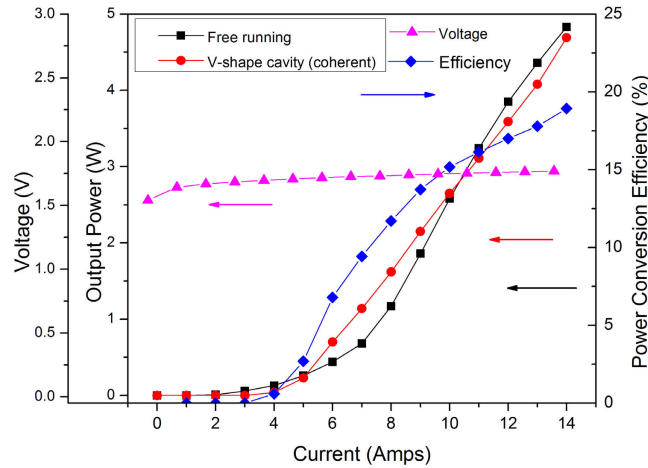


Fig. 5. CW L-I characteristic of coherent beam combining of selected BALD array with an improved external Talbot cavity (red dot-line), CW L-I characteristic of solitary BALD array (black square-line), V-I curve of BALD array (magenta triangle-line) and calculated PCE curve (blue diamond-line) are shown. The power conversion efficiency (PCE) is around 19% at 14 Amps with well-maintained coherent visibility (95%) (See Fig. 8.).

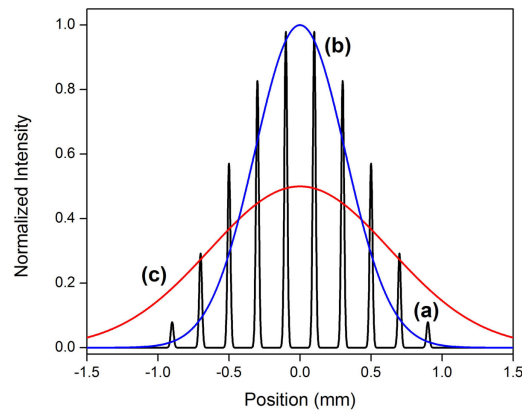


Fig. 6. Calculated diffraction profile of single LD at different position (half Talbot and Talbot distance) and near-field in-phase super-mode distribution of 10 LDs. (a) Near-field of 10 LDs in-phase super mode profile (black line). (b) Diffraction profile of single LD at half Talbot distance with the emission mode size $40 \mu\text{m}$ (blue line). (c) Diffraction profile of single LD at Talbot distance with the emission mode size $40 \mu\text{m}$ (red line). The diffraction profiles of single LD are normalized to the maximum of diffraction at half-Talbot distance.

In our experiment, the emission mode size of LDs is different from single mode LDs [18, 19]. As a result, the diffraction coupling range and relative coupling strength are different. In order to elucidate the diffraction coupling range and relative coupling strength we calculated the diffraction profile of a single LD with broad emission mode at two different positions, i.e. at half-Talbot distance and at Talbot distance. The diffraction profiles of single LD at half-Talbot and Talbot positions are shown in Fig. 6. The near-field of 10 LDs in-phase super-mode is also shown in Fig. 6 in order to compare the optical field overlapping with the diffraction profiles of single LD. The in-phase super-mode can be written

$$\text{as: } E(x, z=0) = \sum_{i=1}^N \sin(k\pi/(N+1)) \exp\left(-((x-x_i)/w)^2\right),$$

where N is the number of

emitters, w is the mode size of emitter, and x_i is the position of emitter [47–49]. In our calculations, we used the parameters from our experiment: the pitch of array ($d = 200 \mu\text{m}$), the emission mode size ($40 \mu\text{m}$, emission mode size is altered with V-shaped feedback), and center wavelength ($\lambda = 800 \text{ nm}$). The diffraction profiles are normalized to be compared with the near-field of 10 LDs. The diffraction profile of single LD when the round trip of external grating cavity is half-Talbot distance (grating is at a quarter of Talbot distance from diodes) overlaps only 4~5 LDs and does not couple all the diodes in the array. On the other hand, the diffraction profile of a single LD when the round trip of external cavity is Talbot distance (grating is at half Talbot distance from diodes) covers the near-field of all 10 LDs. Therefore, when the grating is placed at the half of Talbot distance from diodes, all the 10 LDs are coupled together by the self-image diffraction coupling feedback from the grating at Talbot plane. This creates global coupling structure of the entire array. Additional improvement in mode discrimination is made by tilting the grating by an angle ($\lambda/2d$), where d is the pitch of array [40]. In our experiment, phase locking of 10 LDs was realized when grating was placed at the half Talbot distance and consequently enabled global coupling of the entire array. When we shifted the grating position to the quarter Talbot distance from CL4 image plane (round trip equals half Talbot distance), we did not observe interference fringes at far-field.

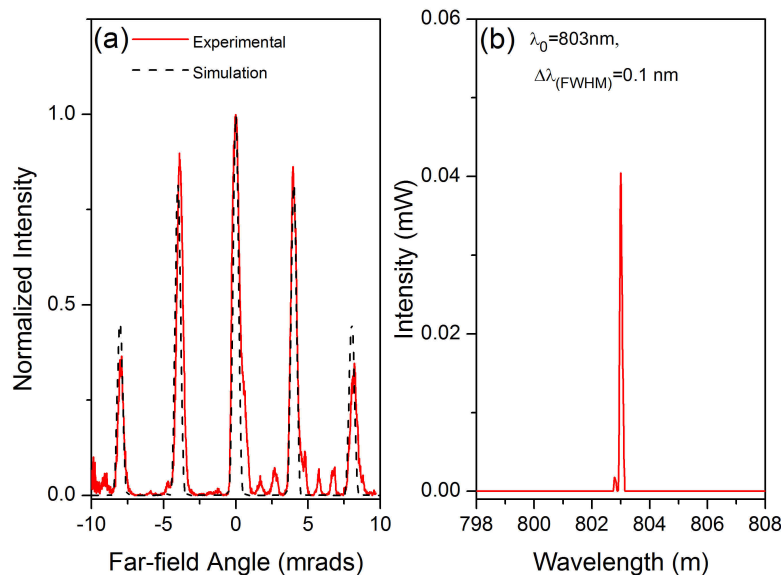


Fig. 7. Experimental results of (a) far-field profile with simulation (dash line) and (b) spectrum of a phase-locked laser array at 5 Å with an improved V-shaped external Talbot cavity.

In [47], D. Mephuys *et. al.*, gave the modal analysis of single mode LDs Talbot cavity and pointed out that quarter Talbot cavity (cavity round trip is equal to half Talbot distance) had the best mode discrimination. Following analysis of D. Mephuys *et. al.* [47], experiments were performed where grating was placed at quarter Talbot distance (cavity round trip is half Talbot distance) [14, 18, 19]. In these experiments, additional improvement in mode discrimination between the in-phase and out-of-phase modes was achieved due to an angle (λ/d) feedback, where d is the pitch of array [18, 19]. For the case where cavity round trip equals Talbot distance (grating from diodes distance is half Talbot distance), mode discrimination was weak. With the external mode discrimination, external half Talbot cavity diode lasers also show high visibility coherent far-field pattern [11]. In our experiment, the extra mode discrimination was achieved by tilting grating an angle ($\lambda/2d$), where d is the pitch of array [40].

The far-field patterns (coherent interference fringes) and spectrum of coherent beam combining of array of 10 BALDs are demonstrated in Figs. 7 and 8 respectively for 5 A and 14 A driven BALD arrays. The visibility of coherent interference fringe is calculated using the following expression: ($V = (I_{\max} - I_{\min}) / (I_{\max} + I_{\min})$), where I_{\max} and I_{\min} are maximum and minimum intensities, respectively. The coherent visibility is around 99% for low drive current (5 A) and ~95% for high drive current (14 A). The spectral line-width (FWHM) of the array is 0.1 nm for both cases (5 A and 14 A). The simulated coherent superposition far-field profile of in-phase locked 10 BALDs (in-phase super-mode) is shown using the dash-line in Fig. 7 and 8. The experimental far-field pattern is well matched with the simulated results. In Fig. 7, the FWHM of each lobe at far-field is 0.6 mrad, which is very close to the numerically simulated angular diffraction limited (0.4 mrad) for 5 A drive (1.5 times diffraction limited). In Fig. 8, the FWHM of 4 out of 5 lobes are 0.64 mrad, which is 1.6 times angular diffraction limited, except for the far left lobe that was 2.1 times diffraction limited. Even though the transverse mode of BALD is controlled by the V-shaped external cavity, a multi-transverse mode emission from BALD is unavoidable due to imperfect AR-coating and high current drive (14 A). As a result, the visibility of interference fringes decreased and some power (16.5% of the total power) was measured in between far-field lobes. However, 83.5% of total power remained in the far-field lobes (interference fringes). Lowering AR-coating values for BALD array in V-shaped external cavity could further reduce multi-transverse mode excitation.

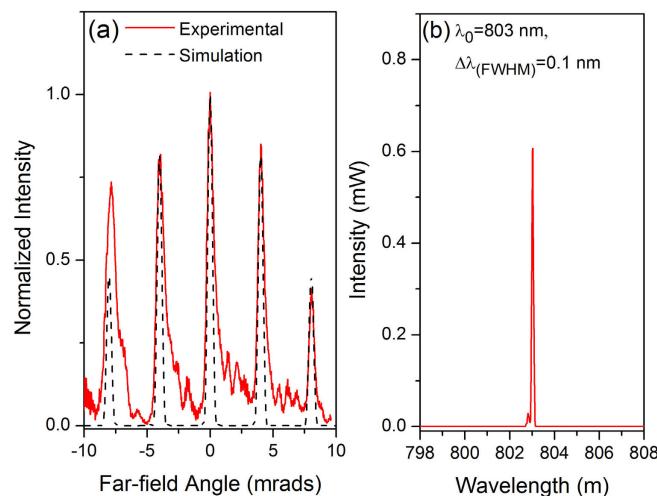


Fig. 8. Experimental results of (a) far-field profile (simulation (dash line)) and (b) spectrum of a phase-locked laser array at 14 A with an improved V-shaped external Talbot cavity.

Near diffraction angular limit far-field indicates that the phases of all the diodes in the BALD array are well locked. Demonstration of near diffraction angular limit coherent beam combining from BALD array indicates that the design-improved V-shaped external cavity provides an excellent mode control of the low AR-coated, low-“smile” BALD array. To the best of our knowledge, near diffraction angular limited coherent emission from BALD array has not been demonstrated in the past. High quality phase locking provides the opportunity of combining all far-field lobes into one beam for future experiments with the approach combined phase shifter and Dammann grating [50].

4. Conclusion

In conclusion, we explored a path of achieving high quality passive phase-locking of high-power BALD array with high PCE. Design-improved V-shape cavity that enabled global coupling among diodes was implemented and we employed low smile, low front-facet AR-coated array of 10 BALDs. We demonstrated 19% PCE at coherent beam combining with well-maintained coherence (high visibility ~95%). Near diffraction angular limited far-field patterns were matched with numerically simulated diffraction patterns of in-phase locked 10 LDs. The far-field angle at the main lobe was measured 1.5 times diffraction limited at low power operation (5A) and 1.6 times diffraction limited at high power operation (14A).

Achieving high quality phase locking with increased PCE requires implementation of single mode control for each laser and properly coupling lasers in array (i.e. properly choosing laser coupling strength and laser coupling topology). This requires reducing reflectivity of AR-coating and “smile” of diode array. The reflectivity of AR-coatings strongly affects the transverse mode selection of BALD in V-shaped external cavity. Optical coupling among laser diodes is significantly affected by the “smile” of BALD array and it is possible to select low smile BALD array [42]. Moreover, the smile correction technology became recently available [51–53]. Considering all the argumentation above, we believe that power scaling of coherent beam combining of BALD arrays is possible.

Acknowledgment

This research was supported in part by the Office of Naval Research and by the Laboratory Directed Research and Development Program of Oak Ridge National Laboratory. Oak Ridge National Laboratory is managed by UT-Battelle, LLC for the U.S. Department of Energy under Contract DE-AC05-00OR22725. Y. B would like to acknowledge NSF support under grant EFRI#1024660.